Validation of VERDICT MRI using fresh and fixed prostate specimens with aligned histological slices

Colleen Bailey[1], Roger M Bourne[2], Bernard Siow[3,4], Edward W Johnston[5], Hayley Pye[6,7], Susan Heavey[6,7], Thomy Mertzanidou[1], Hayley Whitaker[6], Alexander Freeman[8], Dominic Patel[8], Greg Shaw[6,7], Ashwin Sridhar[6,7], Shonit Punwani[5], David J Hawkes[1], Daniel C Alexander[1], and Eleftheria Panagiotaki[1]

[1]Centre for Medical Image Computing, University College London, London, United Kingdom, [2]Discipline of Medical Radiation Sciences, University of Syney, Sydney, Australia, [3]Centre for Advianced Biomedical Imaging, University College London, London, United Kingdom, [4]Imaging, Francis Crick Insitute, London, United Kingdom, [5]Centre for Medical Imaging, University College London, London, United Kingdom, [6]Division of Surgery and Interventional Science, University College London, London, United Kingdom, [7]Department of Urology, University College London Hospitals, London, United Kingdom, [8]Department of Research Pathology, University College London, London, United Kingdom

Synopsis

This study provides the first step in validating the VERDICT diffusion model of tissue microstructure by examining the effects of fixation on tissue microstructure and comparing VERDICT parameter maps to histological features. Fresh and fixed parameter maps showed similar spatial trends: fixation decreased the extracellular volume fraction parameter and decreased the cell radius parameter slightly, consistent with water efflux. Intracellular volume fraction was lower in regions with lower cellularity, such as the peripheral zone, and directions of diffusion anisotropy corresponded with collagen and smooth muscle orientation patterns in the stroma.

Purpose

Biophysical models like VERDICT[1,2] successfully distinguish benign from malignant prostate tissue *in vivo*, but the accuracy with which model parameters reflect the underlying tissue characteristics is unknown. Traditional histology, which is often used as the gold standard for validation, suffers from fixation effects. This study proposes a method to mitigate this problem by comparing VERDICT parameters in fresh and fixed prostatectomy specimens before comparison with corresponding histological slices.

Methods

Specimens

Two prostatectomy specimens were scanned fresh (within 8 hours of surgery) and following formalin fixation (~24 hours later). Fixed specimens were rehydrated for ~10 hours in saline.

Scan protocol

MRI scans were carried out at 9.4 T (Varian Inc). All diffusion images used a PGSE sequence with 1.25 x 1.25 x 2.5 mm^3 resolution. Diffusion scan parameters are listed in Table 1 (3 orthogonal directions + 1 unweighted image each). Additionally, high-angular resolution DWIs (b=938 s/mm^2) were acquired (20 directions fresh, 30 directions fixed). The fresh protocol contained fewer points (VERDICT parameters agreed within 10%, except D_I, which has greater variability for the fresh protocol).

Data analysis

Models combining VERDICT compartments with different shapes were fitted voxelwise[3]. Compartments: Ball (unrestricted isotropic diffusion), Tensor (unrestricted anisotropic diffusion described by three directions), Zeppelin (cylindrically symmetric tensor) and Sphere (isotropically restricted diffusion).

Parameters fitted include the intracellular volume fraction (f_I), intracellular diffusion coefficient (D_I), perpendicular diffusion coefficients ($D_{\perp 1}$, $D_{\perp 2}$), sphere radius (R), and the directions for anisotropic components. The normalization constant and T2 were also fitted. The primary extracellular diffusion coefficient (D_E) was fixed to 1.5 $\mu m^2/ms$.

Model selection used the Akaike Information Criterion, $AIC = -2\ln(L) + 2k$, where L is the maximum likelihood obtained from the fit and k is the number of parameters.

Landmarks in a 3D-printed mold were used to select the same slice for fresh and fixed scans, then aligning by manual rotation and translation.

Histology

Guides in the 3D mold were used to cut 3 µm-sections 5 mm apart, aligned with the imaging plane. Slices were stained with H&E, then digitised (Hamamatsu NanoZoomer) using a 20x objective.

Results and Discussion

Figure 1 shows fits for a voxel with restriction. The Tensor-Ball model did not capture the trends at high b-values (explanation in Figure caption). The data also indicated anisotropy (Fig 1 right), previously observed *ex vivo*[4].

Model selection (via lowest AIC) output is shown in Figure 2. Fresh specimens displayed some voxels where models without restriction (Ball-Ball and Tensor-Ball) were selected. The smaller number of points in the fresh protocol, particularly at high b-values, may reduce the sensitivity to restriction effects. In fixed specimens, the Zeppelin-Sphere and Tensor-Sphere models best explained the data in most voxels, consistent with other studies[4].

Figure 3 shows the effects of fixation on Tensor-Sphere parameters. Spatial trends were similar between fresh and fixed specimens. R was larger in fresh specimens and f_I was smaller, an additional reason that models without restriction may be selected more frequently for fresh tissue: less water experienced the sphere boundary during measurement, which limited the precision of R. The changes in R and f_I may result from an efflux of water and cell shrinkage during fixation.

The extracellular perpendicular diffusion coefficients increased slightly from fresh to fixed (a decrease in anisotropy). The apparent decrease in D_I from 0.63 to 0.22 μm^2/ms may be due to the lower precision of this parameter in the fresh protocol, but the value from fixed voxels agreed with previous high-resolution studies[4].

Figure 4 aligns the f_I and R fixed parameter maps with histology. The zoomed portion for Specimen 1 highlights trends that can be seen across the sample: regions with lower cellularity had lower f_I and R hit the upper limit allowed by the fit in more voxels compared to the transition zone.

The colour FA map indicates the primary diffusion direction and demonstrated stronger anisotropy in stromal regions. The orientation of the collagen and smooth muscle aligned with the primary diffusion direction, a correspondence previously observed using a simple diffusion tensor model[6].

Conclusions

Microstructural features from histology corresponded to features of the VERDICT parameter maps, including fewer cells in regions with low f_I, such as the peripheral zone, and orientation patterns in the stromal regions that corresponded to the orientation of the extracellular anisotropy. Small changes in f_I and R, which can be explained by water efflux, were observed between fresh and fixed tissue maps, but relative trends within a specimen were unaffected. The next step for validation involves clinical VERDICT data and these results emphasise that comparison needs to account for the effects of tissue fixation on microstructure.

Acknowledgements

This work was supported by funding from EPSRC platform grant EP/M020533/1, the CRUK-EPSRC Cancer Imaging Centre at KCL/UCL and by EPSRC fellowship EP/N021967/1.

References

1. Panagiotaki, E. et al. Noninvasive quantification of solid tumor microstructure using VERDICT MRI. Cancer Res. 74, 1902–1912 (2014).

2. Panagiotaki, E. et al. Microstructural Characterization of Normal and Malignant Human Prostate Tissue With Vascular , Extracellular , and Restricted Diffusion for Cytometry in Tumours Magnetic Resonance Imaging. Invest. Radiol. 50, 218–227 (2015).

3. Panagiotaki, E. et al. Compartment models of the diffusion MR signal in brain white matter: a taxonomy and comparison. Neuroimage 59, 2241–54 (2012).

4. Liang, S. et al. Information-based ranking of 10 compartment models of diffusion-weighted signal attenuation in fixed prostate tissue. NMR Biomed. 29, 660-671 (2016).

5. Bourne, R. M. et al. Effect of formalin fixation on biexponential modeling of diffusion decay in prostate tissue. Magn. Reson. Med. 70, 1160–6 (2013).

6. Bourne, R. M., Bongers, A., Chatterjee, A., Sved, P. & Watson, G. Diffusion anisotropy in fresh and fixed prostate tissue ex vivo. Magn. Reson. Med. 634, 626–634 (2015).

Figures

Δ/TE (ms)	δ (ms)	G (mT/m)									
		40	80	120	160	200	240	280	320	360	400
10/19	3 Fresh	9			148		334		594	752	
	Fixed	9		84		232		455		752	928
30/46	3 Fresh	30	120		478		1077 (2)				
	Fixed	30		269		748 (2)		1465 (2)			
	10 Fresh	306	1222	2750		7638 (2)		14971 (2)			
	Fixed	306		2750		7638 (2)		14971 (2)			
50/66	3 Fresh	51	202		808 (2)						
	Fixed	51		455		1263 (4)					
	10 Fresh	535	2139		8555 (4)						
	Fixed	535		4812		13367 (4)					
70/86	3 Fixed	71		640 (2)		1779 (6)					
	10 Fixed	764		6875 (2)		19096 (6)					

Table 1 Scan parameters for the fresh and fixed protocols. The value in each gradient separation (Δ) + duration (δ)/gradient strength (G) box corresponds to the b-value (s/mm^2) for that scan. Empty boxes indicate that gradient strength was not included in the protocol. Values in parentheses show the number of averages for a particular scan (no parentheses=1 average).

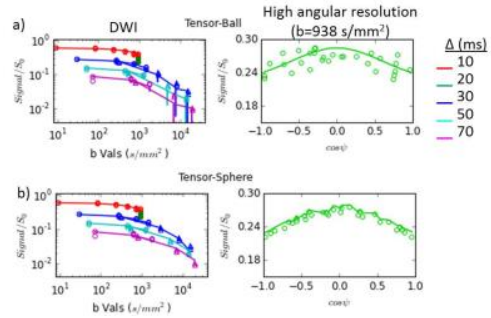

Figure 1 Data (points) with fits (lines) using (a) the Tensor-Ball and (b) Tensor-Sphere models. Left graphs plot signal attenuation with b-value for different Δ. Vertical lines in (a) result from an incorrect primary diffusion direction that attempts to compensate for mis-fit of high-b data for Tensor-Ball. Right graphs plot signal variation with gradient direction for the high angular resolution scan. ψ is the angle between the diffusion gradient and primary diffusion direction of the model (this may differ for different fits, which is why the points have different positions along the x-axes in the top and bottom right plots).

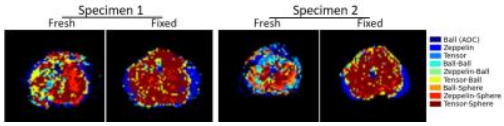

Figure 2 Results of the model selection using the AIC. Zeppelin-Sphere and Tensor-Sphere best explained the data in most voxels of the fixed specimens. Some voxels in the fresh specimens are best explained by models without restriction, as discussed in the text.

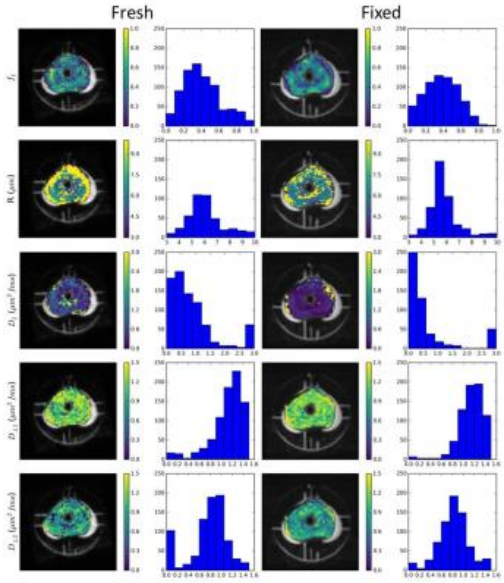

Figure 3 Parametric maps and histograms for all voxels in the prostate for one specimen, fresh (left) and fixed (right). The fresh specimen contains voxels where R hits the maximum of 20 μm allowed by the fit, particularly in the low-cellularity peripheral zone, indicating restriction could not be reliably modelled; these regions correspond to the regions where Ball-Ball and Tensor-Ball are selected in Fig 2. Trends were similar in the second specimen.

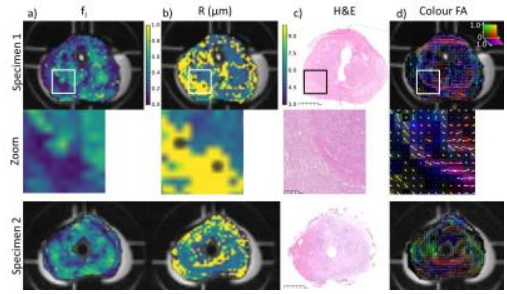

Figure 4 (a) Intracellular volume fraction, f_i, and (b) cell radius, R, maps from the fixed MRI alongside (c) histology for the corresponding slice. (d) The colour FA map for the Tensor portion of the Tensor-Sphere model indicates the primary diffusion direction, with colour and brightness corresponding to the directions and strength of the anisotropy as indicated in the legend at the top right. The boxes on Specimen 1 indicate the zoomed region displayed in the middle row, demonstrating variations in cellularity, collagen alignment and lumen space on histology.